Heat Recovery Systems & CHP Vol. 13, No. 5, pp. 451–461, 1993
Printed in Great Britain

0890-4332/93 $6.00 + .00
Pergamon Press Ltd

PERFORMANCE ANALYSIS OF CAPACITY CONTROL DEVICES FOR HEAT PUMP RECIPROCATING COMPRESSORS

E. PEREIRA PARREIRA* and J. A. R. PARISE†‡
*Universidade Federal de Uberlandia, 38400 Uberlandia, Brazil; and
†Pontificia Universidade Catolica do Rio de Janeiro, 22453 Rio de Janeiro, Brazil

(*Received* 30 *September* 1992)

Abstract—The present paper is concerned with the study of the application of capacity control devices on heat pump reciprocating compressors. Five typical control systems have been studied: variable speed, variable clearance volume, by-pass of the discharge gas, throttling of the suction gas and suction valve cut-off. A simulation model was developed for the analysis. The heating coefficient of performance and the compressor discharge temperature were chosen for the comparison between these five mechanisms. Model predictions revealed that variable speed and variable clearance volume should present the best results. Worst performances went to suction throttling and discharge gas by-passing, both of which present highly irreversible processes.

NOMENCLATURE

A	area (m^2)
C_d	discharge coefficient
C_D	drag coefficient
c_p	specific heat at constant pressure (kJ kg K^{-1})
c_v	damping coefficient (kg s^{-1})
D	compressor cylinder bore (m)
F	force (N)
F_{pl}	valve pre-load (N)
g	gravity acceleration (m s^{-2})
h	specific enthalphy (kJ kg^{-1})
h_r	function that calculates the specific enthalpy in terms of T and P [25] (kJ kg^{-1})
k_s	spring stiffness (N m^{-1})
L	connecting rod length (m)
m	mass (kg)
$\dot{m}$	mass flow rate (kg s^{-1})
P	pressure (N m^{-2})
$\dot{Q}$	rate of heat transfer (kW)
r	crank radius (m)
R	"instantaneous" specific gas constant (kJ kg K^{-1})
t	time (s)
T	temperature (K)
U	internal energy (kJ)
v	specific volume (m^3 kg^{-1})
v_v	function that calculates the specific volume in terms of T and P [25] (m^3 kg^{-1})
V	volume (m^3)
x	effective length of the clearance volume (m)
y	valve displacement (m)
Z_{cv}	valve cut-off ratio
Z_{st}	throttling ratio
Z_{bp}	by-pass ratio

Greek symbols

α	heat transfer coefficient (kW m^2 K^{-1})
γ	specific heat ratio
ΔT_m	logarithmic mean overall temperature difference
θ	crank-angle (degrees)
θ_{sc}	suction valve normal closing angle (degrees)
θ_{sf}	suction valve cut-off angle (degrees)
θ_{so}	suction valve opening angle (degrees)
λ	valve movement binary coefficient
ω	rotational speed (rad s^{-1})

‡Author to whom correspondence should be addressed.

Subscripts

c	saturation conditions at condenser
d	compressor discharge
e	evaporator outlet
i	refrigerant crossing compressor boundaries
l	liquid refrigerant at condenser outlet
s	compressor suction
v	vapor
w	compressor cylinder heat transfer surface
wi	inlet condenser water
wo	outlet condenser water
1	upstream of compressor valve (either suction or discharge)
2	downstream of compressor valve (suction or discharge)

1. INTRODUCTION

Capacity modulation of reciprocating compressors has been the subject of intensive development in the last two decades. The adjustment of compressor throughput, at low cost and reliably, to the varying demands of plants in the process and manufacturing industries has now become a necessity. One particular application of reciprocating compressors concerns refrigeration and heat pump systems. The heat pump can be regarded as a variation of the refrigeration plant, with interest being centered on the delivery of heat at the condenser, rather than in the extraction of heat so as to sustain sub-atmospheric temperatures at the evaporator. Nonetheless the basic thermodynamic cycle (vapor compression) is the same for both systems. A feature of heat pump operation is that the temperature difference between the heat source and heat sink is likely to be more variable than in refrigeration. This results in a wider range of inlet and delivery pressures for the compressor. The thermal load from the heat source is also likely to vary considerably [1]. As a result, compressor capacity modulation becomes almost an essential part of the heat pump operation. The objective of the present paper is to study the application of capacity control devices on heat pump reciprocating compressors.

There are a great variety of compressor capacity control devices available and a number of surveys can be found in the literature [2, 3]. According to Verma [3] capacity modulation can be divided in three basic groups: stepped, stepless and composite control. This is only one criterion as they may be grouped in terms of internal or external control [2], or in regard to the point of application (suction/discharge valve, cylinder volume or drive actuating control). In addition to the traditional start–stop regulation the following devices are studied in the literature: compressor uncoupling, variable speed [4], variable clearance volume [5, 6], variable cylinder volume [7], suction valve cut-off [8], suction valve unloading [9–11], blocked suction [12], top head unloading (internal gas by-passing) [13, 14], suction throttling [15], discharge gas by-passing [15]. The list is not complete as there are a number of variations and combinations of the basic devices [2]. The subject is further reported by Cohen *et al.* [16] and Cohen [17].

In the present paper a numerical simulation model is employed to analyze five devices: variable speed, variable clearance volume, by-pass of the discharge gas, throttling of the suction gas and suction valve cut-off. To find the most suitable device several aspects should be taken into account. They would include the energy conversion efficiency, type of application, cost and reliability, to name but a few. Therefore, it should be stressed that the objective of this paper is restricted to the thermodynamic performance of the devices. A similar analysis has been carried out by Haseltine and Qvale [15] for three different capacity reduction methods. Conclusions were restricted by the simplifications made on the compressor model. As far as capacity control in heat pumps is concerned, the majority of the papers [18–22] concentrate on variable compressor speed.

2. SIMULATION MODEL

The heat pump under consideration is presented schematically in Fig. 1. It is of the vapor compression type and consists of an open-type reciprocating compressor, a water-cooled condenser, evaporator and expansion valve. For the purposes of the present study, it is assumed that the evaporator operates at constant pressure, supplying vapor at a constant degree of superheat.

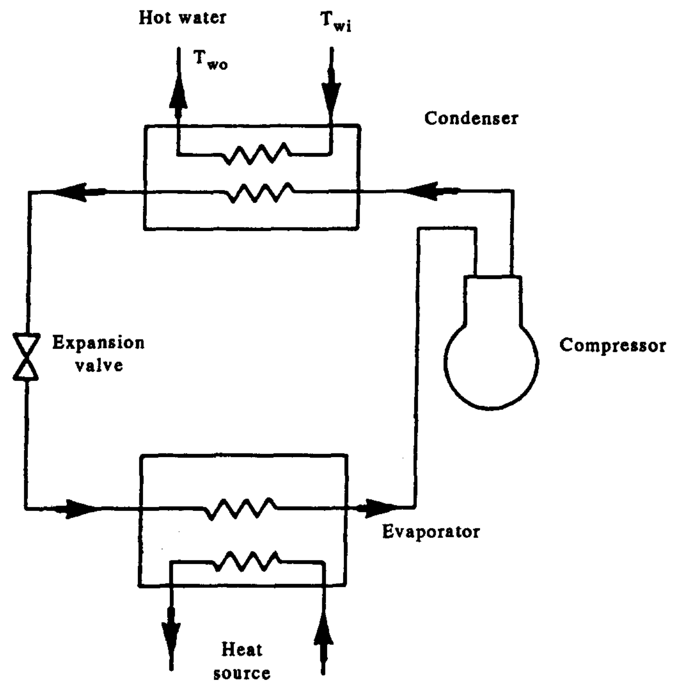

Fig. 1. Vapor compression heat pump.

This assumption limits the simulation to the compressor and condenser unit. Therefore, vapor conditions at the compressor inlet are supplied to the model as input data. In addition to having a less complex model, the reason for this simplification was that it allowed the study of the sole effect of compressor capacity modulation on the condenser water outlet temperature.

A description of the mathematical modeling of the compressor, capacity control devices and condenser is presented next.

2.1 *Compressor*

A detailed model for the compressor has been utilized. It follows traditional methods of computer simulation for reciprocating compressors [23] by considering the cylinder space as a control volume (Fig. 2) with two flow boundaries (valves), a moving boundary (piston) and heat transfer across its surface. Full description of the model is given in [24].

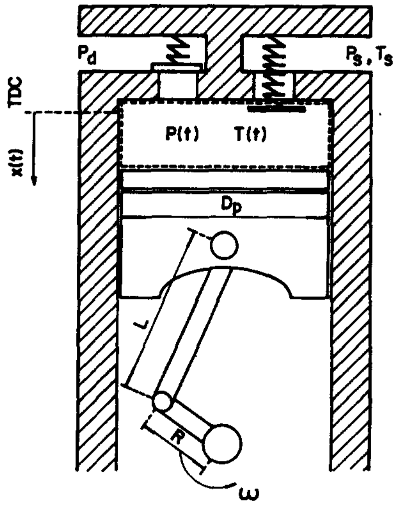

Fig. 2. Compressor volume of control.

The energy equation, in its time-derivative form, is applied to the control volume:

$$\frac{dU}{dt} = h_i \frac{dm}{dt} + \dot{Q} - P\frac{dV}{dt}. \quad (1)$$

Equation (1), after a number of substitutions, becomes:

$$\frac{dp}{dt} = -\frac{1}{V}\left[\dot{Q} - m\frac{dh}{dt} - (h - h_i)\right], \quad (2)$$

where P and V are the instantaneous cylinder pressure and volume and h and m, the gas specific enthalpy and mass. Integration of equation (2) gives the variation of cylinder pressure with time. Subscript "i" refers to the condition of the gas (vapor) crossing the boundaries of the control volume. The continuity equation relates the rate of mass variation inside the cylinder, dm/dt, with the gas mass flow rate across the valve orifices.

Suction valve:

$$\frac{dm}{dt} = \dot{m}; \quad (3)$$

discharge valve:

$$\frac{dm}{dt} = -\dot{m}. \quad (4)$$

Further equations are required for the determination of the right-hand side terms of (2). They are: the heat transfer equation, kinematics equation (V and dV/dt), equation of state (m), enthalpy equation (h) and valve mass flow rate equation (dm/dt). Real gas equations [25], $v = v_v(T, P)$ and $h = h_v(T, P)$, are used for the evaluation of m ($m = V/v$) and h. Pressure fluctuations in the inlet and delivery ducts are ignored, so that evaporating and condensing pressures are considered to be steady throughout the cycle. For the mass flow rate through the valves, one-dimensional flow through a variable orifice area is assumed.

The mass flow rate, for isentropic flow through an orifice of effective area A_f from an upstream condition 1 to state 2, is

$$\dot{m} = A_f P_1 \left[\frac{2\gamma}{(\gamma - 1)RT_1}\left[\left(\frac{P_2}{p_1}\right)^{2/\gamma} - \left(\frac{P_2}{P_1}\right)^{(\gamma+1)/\gamma}\right]\right]. \quad (5)$$

R is regarded as an instantaneous specific gas constant. Its value is obtained by writing the real state equation $\{v = v_v(T, P)\}$ in the form $(R = Pv/T)$. Both R and the specific heat ratio γ are evaluated at the upstream state 1 and, consequently, vary with time.

For compressible flow, the discharge coefficient C_d approximates [24] to

$$C_d = 0.703 + 0.138 \sin\left[\frac{\pi}{2}\left(1 - 1.515\frac{P_1}{P_2}\right)\right]. \quad (6)$$

One original aspect of the model [24] concerns the generalized equation for the effective flow area as related to valve lift, y.

$$A_f = C_D A_{max} \sin\left[\frac{\pi}{2}\left(\frac{y}{y_{max}}\right)\right]. \quad (7)$$

Equation (7) was found to agree well with experimental data from several authors [26–28] (Fig. 3).

The model also requires detailed information on the valve system, which includes: valve and spring masses, spring stiffness, valve pre-load, viscous damping factors, drag and discharge coefficients, maximum displacement and flow areas.

Valve lift and pressure difference are related by the dynamics of valve motion (one degree of freedom model). The valve may be considered as being acted on by four forces. These are: the aerodynamic force caused by pressure difference, the spring force, a viscous damping force, and, finally, the gravitational force. Newton's law of motion applied to the valve gives an equation for the valve lift;

$$m_t\frac{d^2y}{dt^2} + c_y\frac{dy}{dt} + ky = -F_{pl} + \lambda(m_v + m_s)g + C_D A_p \Delta P(t). \quad (8)$$

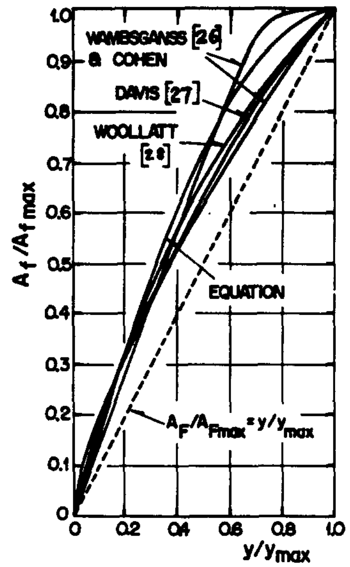

Fig. 3. Valve effective flow area against valve displacement.

The total mass m_t of the valve includes a fraction of the spring mass, c_v is the viscous damping term, k_s is the spring stiffness and F_{pl} is the spring pre-load force when the valve is closed. The pressure difference acting on the projected area A_p of the reed is ΔP and the coefficient C_D, typically 0.8, accounts for the variation of ΔP across the surface of the reed. The sign of the gravitational term $(m_v + m_s)g$, depends on the direction in which the valve opens, and is given by the binary variable λ (equal to 1 or -1). Other forces that may exist, such as valve bouncing at seats and oil stiction, have not been taken into account.

Equation (8) has two time-dependent variables P and y, and is, therefore, coupled to energy and mass flow rate equations. However, considering that the numerical solution progresses in small time-steps (0.5 degrees of crank angle), it is reasonable to assume that $\Delta P(t)$ remains constant throughout any one time interval. Therefore,

$$\Delta P(t) \approx \Delta P. \tag{9}$$

Defining F_v as the sum of all time-independent force components, equation (8) becomes:

$$m_t \frac{\mathrm{d}^2 y}{\mathrm{d}t^2} + c_v \frac{\mathrm{d}y}{\mathrm{d}t} + ky = F_v \tag{10}$$

where

$$F_v = -F_{pl} + \lambda(m_v + m_s)g + C_D A_p \Delta P. \tag{11}$$

Equation (10) can now be solved to give explicit expressions for valve displacement and velocity.

The rate of heat transfer from the cylinder wall at temperature T_w to the gas in the cylinder at temperature T is given by

$$\dot{Q} = \alpha A_w (T_w - T). \tag{12}$$

A_w is the area of the cylinder heat and the fraction of the cylinder wall not covered by the piston; the corresponding value of the heat transfer coefficient varies with piston movement and correlations for its evaluation are provided in the literature [23]. The cylinder wall temperature is regarded as constant and uniform throughout the cycle.

A kinematic equation relates V, t and crank geometry:

$$V(t) = \frac{\pi D^2}{4}\left[x + r(1 - \cos \omega t) + L\left[1 - \sqrt{1 - \left(\frac{r}{L}\sin \omega t\right)^2}\right]\right], \tag{13}$$

where D is cylinder bore, x is the effective length of the clearance volume, r is crank length, L is connecting rod length and ω is the shaft speed.

The equations presented above form a set of coupled ordinary differential equations. The solution procedure adopted was to rearrange the governing equations as expressions for the rate of change of cylinder pressure and temperature. These two rate equations were solved by the fourth-order Runge Kutta method to determine the increment in P and T over each time step (or crank angle increment). With the integration, a complete analysis of the sequence of events occurring in the compressor can be carried out. Input data to the computation includes all relevant dimensions of the compressor, valve characteristics, shaft speed, ambient temperature and heat transfer coefficient to the surroundings. The state of the refrigerant in the inlet manifold must be specified completely but, for the delivery manifold, only pressure needs to be prescribed. The state of the refrigerant within the cylinder is not known initially at any point in the cycle, which requires a few cycle calculations (typically five) in order to achieve convergence. With calculations completed the following parameters are known: compressor power consumption, time-averaged discharge temperature and refrigerant mass flow rate.

Further details of the numerical solution and the validation of the compressor model with experimental data are provided in [24].

2.2 *Capacity control devices*

2.2.1. *Variable speed and variable clearance volume.* There was no need to create a specific mathematical model for these devices as this could be done simply by altering the input data for the compressor subroutine (shaft speed and clearance volume ratio are input values for the compressor subprogram).

2.2.2. *Suction valve cut-off mechanism.* Modeling the suction valve cut-off mechanism was done by imposing an instantaneous closure of the valve (i.e. zero displacement, $y = 0$). To cover the whole range of operation of the suction valve cut-off mechanism, a cut-off ratio, Z_{vc}, was defined as

$$Z_{vc} = \frac{\theta_{sf} - \theta_{so}}{\theta_{sc} - \theta_{so}}, \tag{14}$$

where θ_{sf} is the suction valve cut-off angle, θ_{so} is the opening angle and θ_{sc} is the closure angle should no cut-off mechanism be installed. The model is first run with the suction valve operating normally, so as to provide the values of θ_{so} and θ_{sc}. The cut-off ratio is an input value for the model and is a measure of how early the suction valve is cut-off.

2.2.3. *Suction throttling mechanism.* Energy and mass conservation equations are applied to account for the presence of suction throttling. For the suction throttling set-up, Fig. 4, the throttling ratio, Z_{sc}, was defined as:

$$Z_{st} = \frac{P_s}{P_e}. \tag{15}$$

From equation (15), it can be seen that the condition of full capacity corresponds to Z_{sc} equal to 1, corresponding to no restriction at the compressor suction.

Applying the energy equation to the throttling valve volume of control, one has:

$$h_e = h_s \tag{16}$$

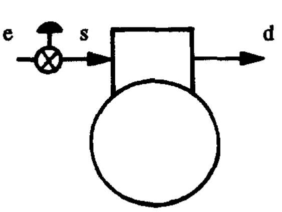

Fig. 4. Suction throttling.

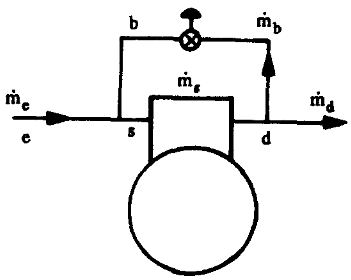

Fig. 5. Discharge gas by-pass.

or

$$h_v(T_e, P_e) = h_v(T_s, P_s), \tag{17}$$

where h_v is a function [25] which provides the specific enthalpy in terms of T and P.

Given the approaching conditions, T_e and P_e, and a prescribed value of Z_{st}, equation (17) can be written schematically as

$$F(T_s) = 0. \tag{18}$$

Solution of equation (18) provides the gas temperature downstream of the throttle valve.

2.2.4. *Gas by-passing mechanism.* The discharge gas by-pass ratio, Z_{bp}, is defined in terms of the existing mass flow rates (Fig. 5).

$$Z_{bp} = 1 - \frac{\dot{m}_b}{\dot{m}_s}. \tag{19}$$

Again, a null by-pass ratio corresponds to the no-flow condition. Mass and energy conservation equations must be applied in order to evaluate the compressor inlet conditions that will result from the prescribed by-pass ratio. The continuity equation provides

$$\dot{m}_e + \dot{m}_b = \dot{m}_s. \tag{20}$$

The energy equation, applied to the merge of the by-pass gas with the stream coming from the evaporator gives

$$m_e h_e + \dot{m}_b = \dot{m}_s h_s. \tag{21}$$

Introducing equations (19) and (20) into (21):

$$Z_{bp} h_e + (1 - Z_{bp}) h_b = h_s. \tag{22}$$

As for conditions downstream of the by-pass valve, which reduces the pressure from discharge to suction levels, one has:

$$h_d = h_b \tag{23}$$

or

$$h_v(T_d, P_d) = h_v(T_b, P_s). \tag{24}$$

The system compressor/by-pass valve is solved iteratively, as follows:

(1) estimate state s, (T_s, P_s);

(2) perform compressor calculation with the compressor subroutine: from (T_s, P_s, P_d) obtain $\dot{m}_s$, T_d and W_{cp};

(3) calculate $\dot{m}_b$ from equation (19);

(4) from equation (23) calculate h_b;

(5) with states b and e, calculate compressor inlet conditions s, equation (22);

(6) return to (2) until convergence on state s is obtained.

2.3 *Condenser*

The condenser is modelled by the usual three heat exchanger equations (heat balances over water and refrigerant streams and the log–mean temperature difference equation).

$$\dot{Q}_c = \dot{m}_d (h_d - h_l) \tag{25}$$

$$\dot{Q}_c = \dot{m}_w c_{pw} (T_{wo} - T_{wi}) \tag{26}$$

$$\dot{Q}_c = U_c A_c \Delta T_m. \tag{27}$$

The mean temperature difference, assuming no sub-cooling at the condenser exit, is approximated by

$$\Delta T_m = \frac{(T_d - T_{wo}) - (T_c - T_{wi})}{\ln\left[\dfrac{(T_d - T_{wo})}{(T_c - T_{wi})}\right]}. \tag{28}$$

Table 1. Characteristics of the compressor suction and discharge valves

Characteristics	Suction valve	Discharge valve
Valve mass	0.005516 kg	0.00363 kg
Spring mass	0.0 kg	0.00189 kg
Spring stiffness	0.2033×10^{4} N m^{-1}	0.333×10^{-3} N m^{-1}
Spring pre-load	0 N	4.3 N
Damping factor	0.005	0.005
Drag coefficient	0.3	0.8
Valve force area	0.6535×10^{-3} m^2	0.4838×10^{-3} m^2
Maximum flow area	0.725×10^{-2} m^2	0.3556×10^{-3} m^2
Maximum lift		0.4225×10^{-2} m

2.4 *Solution*

For the modeling of the compressor/condenser unit the following algorithm is presented:

(a) With suction conditions (T_s and P_s) and an estimated discharge pressure, P_d, perform the capacity controlled compressor model, in order to provide the refrigerant mass flow rate and compressor discharge temperature.

(b) From condenser inlet conditions, *d*, determine the condensing and water outlet temperatures, T_c and T_{wo}, and the thermal power output Q_c.

(c) Compare the estimated condensing pressure P_c with that used for the compressor model (P_d).

(d) If convergence in P_c has not been achieved return to (a) with a new value.

3. RESULTS AND DISCUSSION

The model was applied to a typical medium-sized heat pump system. A two-cylinder compressor operated at a nominal speed of 1500 rpm, with suction at 283 K and 3 bar. The clearance ratio was set at 0.0363 with a bore/stroke of 0.0667/0.0635 m. The condenser was assumed to have an overall heat transfer coefficient of 0.4 kW K^{-1} and 2 m^2 of transfer area. Water inlet temperature was kept at 303 K at a mass flow rate of 0.154 kg s^{-1}. Refrigerant-12 was taken as the working fluid. Table 1 gives the characteristics of the compressor valving system.

In the first comparative analysis (Figs 6–9), the compressor was supposed to run at a constant pressure ratio of 5, with the mass flow rate ranging from 100 to 30% (mass flow ratio of 0.3) of the design point. For this study only the compressor model was utilized.

Figure 6 depicts the variation of the volumetric efficiency with the mass flow ratio. It can be seen that three of the capacity control devices (suction throttling, variable clearance volume and suction valve cut-off) do act on the compressor volumetric efficiency. This is not the case for the gas by-passing, as the efficiency is defined in terms of the mass flow rate at the discharge port. As for the variable speed device, lower shaft speeds resulted in reduced gas flow losses, leading to an increase in the volumetric efficiency.

With the exception of gas by-passing, where practically the same quantity of gas must always circulate through the compressor, all devices presented a reduction in power consumption for lower

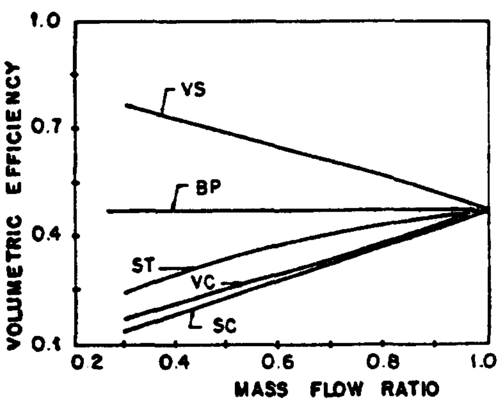

Fig. 6. Effect of capacity control on compressor volumetric efficiency.

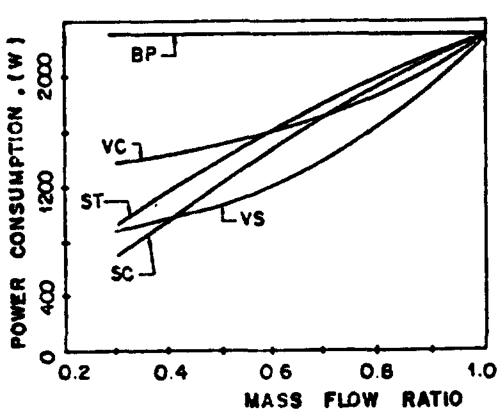

Fig. 7. Effect of capacity control on compressor power consumption.

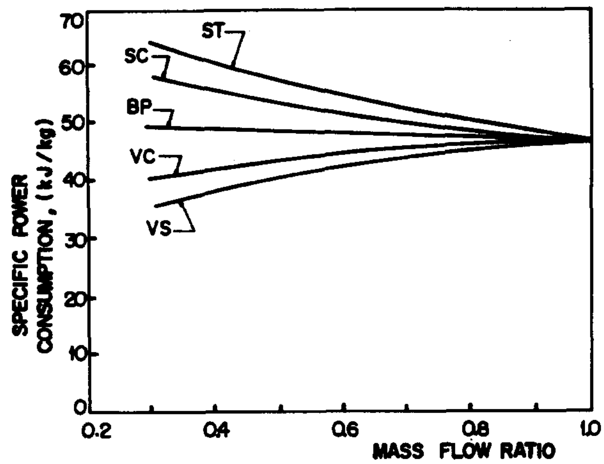

Fig. 8. Effect of capacity control on compressor specific power consumption.

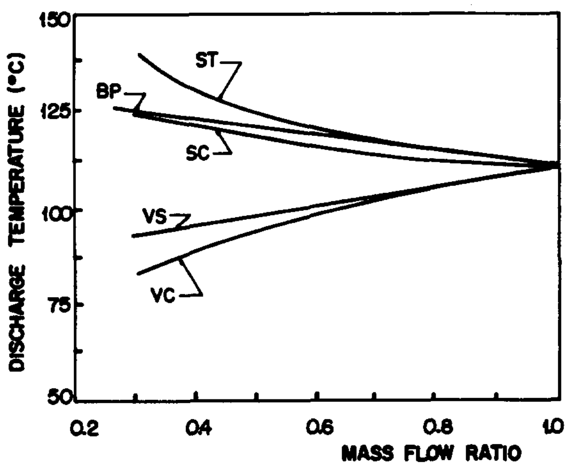

Fig. 9. Effect of capacity control on compressor gas discharge temperature.

mass flow ratios (Fig. 7). However, this situation changes when the comparison is made in terms of the specific power consumption (Watts per kg s^{-1} of gas) (Fig. 8). Variable clearance volume and variable speed stand out as the most effective methods, with suction throttling and suction valve cut-off presenting the worst results. Such behavior will directly affect the heat pump performance.

One important parameter for heat pump applications refers to the compressor discharge temperature, which must not exceed the regrigerant thermal stability limit. Again, Fig. 9, variable clearance volume and variable speed presented, by far, the best results. In fact, the other devices showed a serious tendency to increase the discharge temperature at reduced mass flow ratios. Without a proper design this could jeopardize the entire control effort.

In the second analysis, a model was employed to simulate the operation of the heat pump with three different water flow rates (0.154, 0.24 and 0.49 kg s^{-1}), each providing, at the design point, an outlet temperature of 333 K, 323 K and 313 K, respectively. From the predicted results (Fig. 10) it can be concluded that, in theory, all five devices were able to provide a wide range of condenser outlet temperatures. Water inlet temperature, for all cases in Fig. 10, was 303 K.

Figures 11 and 12 summarize the heat pump analysis, showing the variation of the heating coefficient of performance and the compressor discharge temperature with the condenser water outlet temperature. Clearly, variable clearance volume and variable speed presented the best results: water temperature reduction with an increasing COP and within safe limits for the refrigerant stability. In fact, results from Fig. 11 have been anticipated by Fig. 8, with the difference that the compressor pressure ratio, dependent on the condensing pressure, is now varying. Not surprisingly, the devices

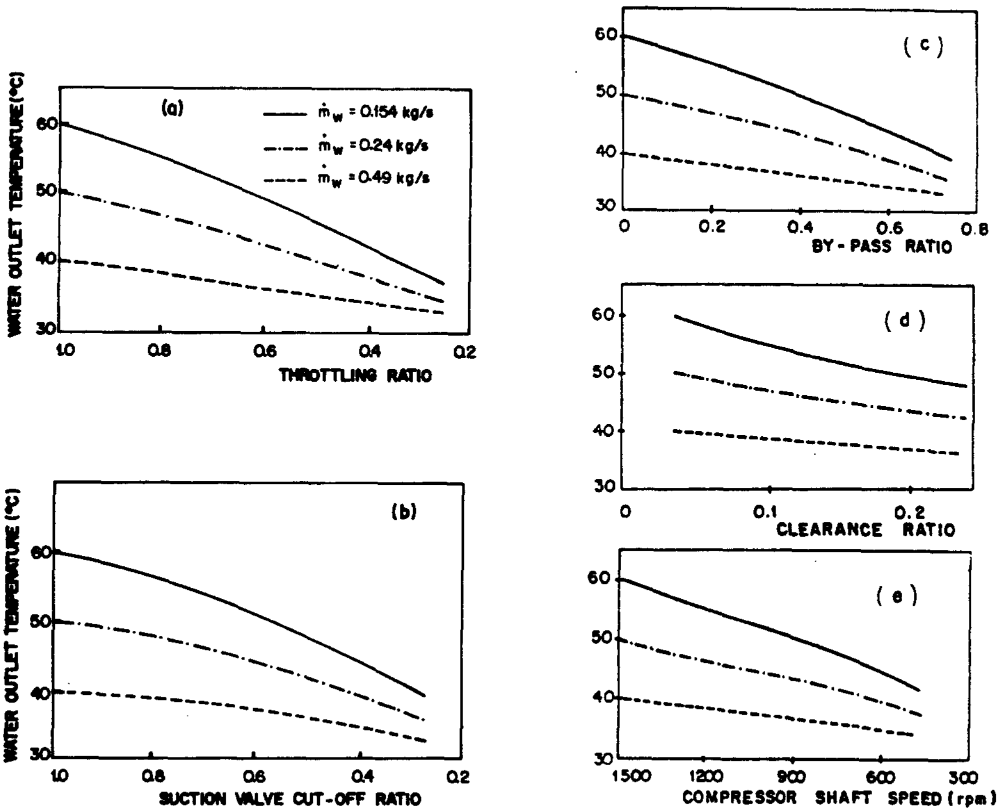

Fig. 10. Control of hot water temperature with: (a) suction throttling; (b) suction valve cut-off; (c) discharge gas by-pass; (d) variable clearance volume; (e) variable shaft speed.

that make use of irreversible processes, such as throttling (ST, BP) and gas mixing (BP), presented the worst performances, not only in respect to the COP but also regarding the temperature levels achieved at the discharge. As for the suction valve cut-off method, COP figures were not adversely affected, even though Fig. 12 shows that the discharge temperature may be cause for concern.

4. CONCLUDING REMARKS

The main objective of the paper was to assess how the condenser water outlet temperature could be controlled by means of varying the compressor capacity. For that a simulation model for the

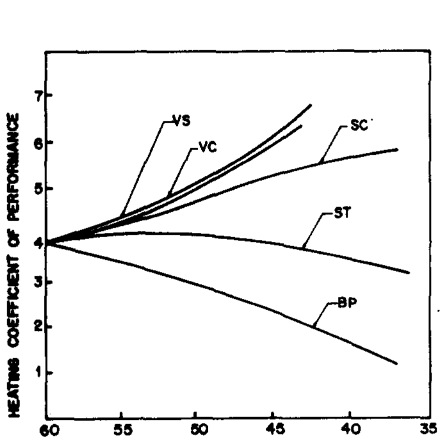

Fig. 11. Heat pump coefficient of performance against condenser water outlet temperature.

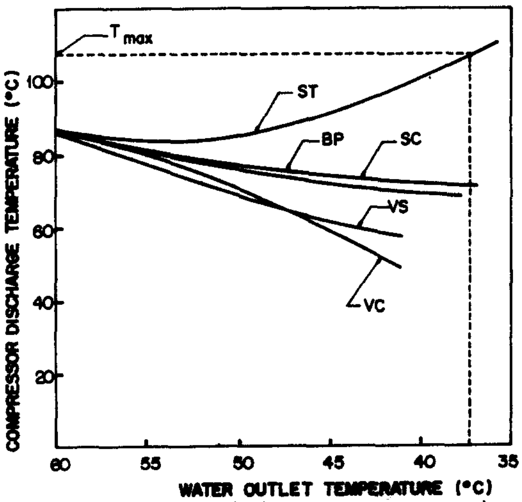

Fig. 12. Compressor discharge temperature against condenser water outlet temperature.

heat pump was developed. It included the model for the compressor itself (with constant intake and delivery pressures, valve dynamics and heat transfer across cylinder walls) as well as a simplified model for the condenser.

To compare all five mechanisms, two parameters have been selected: the heat pump coefficient of performance and the compressor discharge temperature, this one being important in the refrigerant thermal stability aspect. Generally, it has been concluded that best results were obtained with variable speed and variable clearance volume. Suction throttling and discharge gas by-passing, being highly irreversible processes, presented the worst performances.

REFERENCES

1. J. A. R. Parise, Heat pumps: a survey on heat sources. In *Proc. VIII Brazilian Cong. Mech. Eng.*, pp. 213–216. Sao Jose dos Campos, Brazil (1985).
2. H. Holdack-Janssen and H. Kruse, *Continuous and discontinuous capacity control for high speed refrigeration compressors.* In *Proc. Purdue Comp. Tech. Conf.*, pp. 67–75 (1984).
3. J. C. Verma, Optimum utilization of capacity control devices in reciprocating compressors. In *Proc. Purdue Comp. Tech. Conf.*, pp. 509–520 (1986).
4. A. M. Bredensen and J. Paul, Effects of speed control on the valve performance and on the energy efficiency of heat reciprocating compressors. In *Proc. Antriebe fur Warme Pumpen*, West Germany, pp. 69–74 (1979).
5. K. W. Yun and L. Reese, Over-re-expansion as a means of compressor capacity modulation. In *Proc. Purdue Comp. Tech. Conf.*, pp. 61–66 (1984).
6. W. J. Tuymer, Stepless variable capacity control. In *Proc. Purdue Comp. Tech. Conf.*, pp. 61–66 (1974).
7. C. M. Bartolini and G. Vincenzi, New internal capacity control for reciprocating compressors. In *Proc. Purdue Comp. Tech. Conf.*, pp. 521–536 (1986).
8. C. C. Hiller and L. R. Glicksman, Compressor capacity control via early suction valve closing. In *Proc. Purdue Comp. Tech. Conf.*, pp. 137–140 (1976).
9. A. Korsgaard, Automatic capacity regulation of refrigerating compressors. In *Proc. XII Int. Cong. Refrg.*, paper 3.40. Madrid (1967).
10. D. L. Boyd, Capacity control of reciprocating compressors used in refrigeration systems. In *Proc. Purdue Comp. Tech. Conf.*, pp. 37–43 (1972).
11. K. H. White, Infinitely variable capacity control. In *Proc. Purdue Comp. Tech. Conf.*, pp. 47–51 (1971).
12. F. J. Ehrlich, Blocked suction unloading improves part load efficiency of semi-hermetic reciprocating compressor. In *Proc. Purdue Comp. Tech. Conf.*, pp. 56–60 (1986).
13. L. W. Cheney, A new approach to compressor capacity modulation. In *Proc. Purdue Comp. Tech. Conf.*, pp. 55–60 (1974).
14. W. Hartwick, Power requirements and associated effects of reciprocating compressor cylinders ends deactivated by internal by passing. In *Proc. Purdue Comp. Tech. Conf.*, pp. 141–149 (1976).
15. J. D. Haseltine and E. B. Qvale, Comparison of power and efficiency of constant-speed compressors using three different capacity reduction methods, *ASHRAE Trans.* **77** part I, 158–162 (1971).
16. R. Cohen, J. F. Hamilton and J. T. Pearson, Possible energy conservation through use of variable capacity compressor. In *Proc. Purdue Comp. Tech. Conf.*, pp. 50–54 (1974).
17. R. Cohen, Advances in compressor technology (as reported in 1988). *Int. J. Ref.* **13**, 274–277 (1990).
18. C. C. Hiller and L. R. Glicksman, Compressor capacity control. In *Heat Pump Technology for Saving Energy* (edited by M. J. Collie), pp. 276–333. Noyes Data Corp (1979).
19. S. A. Tassou, C. J. Marquand and D. R. Wilson, The effects of capacity modulation on the performance of vapor compression heat pump systems. *Int. Symp. Industrial Application of Heat Pumps*, Warwick, U.K., 187–196, (1982).
20. J. A. R. Parise and W. G. Cartwright, Performance characteristics of a high temperature water-to-water heat pump. *J. Energy Res.* **14**, 647–660 (1988).
21. D. F. Neale, Y. T. Wang, D. R. Wilson, R. K. Green and M. Searle, Microprocessor based control system for heat pumps, *Third Int. Conf. Future Energy Concepts, IEE Conf. 192*, London, pp. 238–241 (1981).
22. H. Holzapfel, V. Brunop and V. Recchi, Experimental analysis of a water-to-water heat pump with variable speed scroll compressor. In *Proc. Purdue Int. Comp. Engng Conf.*, Vol. IV, pp. 1529–1538, 14–17 July (1992).
23. W. Soedel, Introduction to computer simulation of positive displacement type compressor, Short Course Notes, Purdue University, School of Mechanical Engineering, West Lafayette, U.S.A., July (1972).
24. J. A. R. Parise and W. G. Cartwright, Simulation of reciprocating compressors: numerical method and comparison with experimental data. *Revista Brasileira de Ciencias Mecanicas (Journal of the Brazilian Society of Mechanical Sciences)* **VII**, 129–152 (1985).
25. G. W. Gatecliff and E. R. Lady, Explicit representation of the thermodynamic properties of refrigerants 12 and 22 in the superheat region. In *Proc. Purdue Comp. Tech. Conf.*, pp. 287–290 (1974).
26. M. W. Wambsganss Jr. and R. Cohen, Dynamics of reciprocating compressor with automatic reed valves. I: Theory and simulation. II: Experiments and evaluation. In *Proc. XII Int. Cong. Refr.*, paper 3.06. Madrid (1967).
27. D. Wollatt, A simple numerical solution for compressor valves with one degree of freedom. In *Proc. Purdue Comp. Tech. Conf.*, pp. 159–165 (1974).
28. H. Davis, Effects of reciprocating valve design on performance and reliability. In *Proc. Inst. Mech. Engrs Conf. on "Industrial Reciprocating and Rotary Compressors, Design and Operational Problems"*, London, pp. 9–23, October (1970).